The Journal of Chemical Physics

Crystallization growth rates and front propagation in amorphous solid water films

Cite as: J. Chem. Phys. **150**, 214703 (2019); https://doi.org/10.1063/1.5098481
Submitted: 02 April 2019 • Accepted: 14 May 2019 • Published Online: 05 June 2019

R. Scott Smith, Chunqing Yuan, Nikolay G. Petrik, et al.

The Journal of Chemical Physics ARTICLE scitation.org/journal/jcp

Crystallization growth rates and front propagation in amorphous solid water films

Cite as: J. Chem. Phys. 150, 214703 (2019); doi: 10.1063/1.5098481
Submitted: 2 April 2019 • Accepted: 14 May 2019 •
Published Online: 5 June 2019

R. Scott Smith,[a] Chunqing Yuan, Nikolay G. Petrik, Greg A. Kimmel, and Bruce D. Kay[a]

AFFILIATIONS

Physical Sciences Division, Pacific Northwest National Laboratory, Richland, Washington 99352, USA

Note: This paper is part of a JCP Special Topic on Chemical Physics of Supercooled Water.
[a]**Authors to whom correspondence should be addressed:** Scott.Smith@pnnl.gov and Bruce.Kay@pnnl.gov

ABSTRACT

The growth rate of crystalline ice (CI) in amorphous solid water (ASW) films was investigated using reflection absorption infrared spectroscopy. Two different experiments were set up to measure rates of the crystallization front propagation from the underlying crystalline template upward and from the vacuum interface downward. In one set of experiments, layers of ASW (5% D_2O in H_2O) were grown on a CI template and capped with a decane layer. In isothermal experiments from 140 to 150 K, crystallization was observed from the onset (no induction time) and the extent of crystallization increased linearly with time. In a second set of experiments, uncapped ASW films without a CI template were studied. The films were created by placing a 100 ML isotopic layer (5% D_2O in H_2O) at various positions in a 1000 ML ASW (H_2O) film. The CI growth rates obtained from the two configurations (capped films with a CI template and uncapped films without a CI template) are in quantitative agreement. The results support the idea that for ASW films in a vacuum, a crystalline layer forms at the surface that then acts as a CI template for a growth front that moves downward into the film.

I. INTRODUCTION

Amorphous solid water (ASW) has been the subject of research for many reasons including its importance in astrophysical environments[1–4] and its role as a model system in understanding the behavior of supercooled liquid water.[5–16] In the laboratory, ASW can be created in a vacuum chamber by vapor deposition onto a cold substrate (T < 130 K).[9,17] Metastable ASW films will eventually transform to the lower energy crystalline phase where the kinetics will depend on the temperature.

The crystallization kinetics for ASW have been studied by a number of groups using a variety of techniques.[3,4,9,17–32] In many cases, the crystallization kinetics were used to extract nucleation and growth rates for the formation of crystalline ice (CI) from deeply supercooled liquid water.[4,24–26,30,31] The extraction of the nucleation and growth rates from the crystallization kinetics requires knowledge of, or an assumption about, the crystallization mechanism. In most of the prior work, a random bulk nucleation mechanism was used in the analysis.

In some recent work, we probed the role of the vacuum interface in ice nucleation by comparing the isothermal crystallization of 1000 ML ASW films with ("capped") and without ("uncapped") a decane layer on top of the film.[33,34] We found that the crystallization rate for the "uncapped" films was about eight times faster than that for the "capped" films. We also showed that crystallization for "uncapped" films begins at the ASW/vacuum interface. The plausible explanation for more facile surface nucleation is that molecules at the surface are less constrained than those in the bulk and likely have a lower energy barrier for nucleation. A "top-down" crystallization mechanism was proposed in which, once formed, the outer crystalline layer acts as a template that results in a crystallization growth front that propagates into the bulk.

In this paper, we measure the isothermal crystallization kinetics of ASW films in two composite film configurations. In the first configuration, ASW is deposited onto a crystalline ice (CI) template and capped with a decane layer. The decane cap either prevents or significantly retards nucleation of a crystalline ice layer at the outer surface of the film. Furthermore, the CI template eliminates the need for nucleation and ASW crystallizes due to the propagation of the ice front from the template. The crystalline ice growth rate can then be obtained directly from the crystallization kinetics. In the second configuration, uncapped ASW films without a CI template

were studied. In this case, nucleation and growth of crystalline ice at the ASW/vacuum interface also influence the crystallization kinetics. The crystalline ice growth rates obtained from the two configurations (capped films with a CI template and uncapped films without a CI template) are in quantitative agreement. The results support our previously proposed crystallization mechanism for ASW films in a vacuum, where crystallization begins at the vacuum interface, creates a relatively thin crystalline skin or crust across the film, and, once formed, the crystallization front moves through the ASW film.[33,34]

II. EXPERIMENTAL

The crystallization kinetics were studied using a previously described ultrahigh vacuum chamber (UHV, base pressure $<10^{-10}$ Torr) that is coupled to an FTIR spectrometer for reflection absorption infrared spectroscopy (RAIRS) experiments.[22,35] The ASW films were created by molecular beam deposition onto a 1 cm diameter graphene covered Pt(111) substrate at normal incidence at ~25 K. The Pt(111) single crystal was heated to 1100 K and exposed to a beam of decane to create the graphene overlayer.[36] We used a graphene covered Pt(111) as a substrate for convenience because we have found that it remains clean and ordered with respect to repeated dose and desorption cycles. Resistive heating using two tantalum wires spot welded to the backside of the Pt(111) and a closed cycle helium cryostat were used to control the temperature of the sample. A K-type thermocouple spot-welded to the backside the Pt(111) substrate was used to measure the temperature. We estimated the reported temperature to have a precision of better than ±0.01 K and an absolute accuracy of ±2 K. The water (neat H_2O and 5% D_2O in H_2O liquid) films were deposited on top of and in some cases capped with 50 ML of decane. In a 5% D_2O in H_2O solution, the D_2O will react to form HDO. In a dilute HDO mixture, the O-D stretch is decoupled from the OH stretches and this facilitates the analysis of ASW crystallization kinetics.[37,38] The deposition fluxes were 0.87 ML/s for water and 0.48 ML/s for decane. The crystalline template was created by depositing an ASW film at 25 K, heating to 150 K for 150 s, and then cooling back to 25 K. The initial dose was adjusted to account for desorption so that the template had a final thickness of 50 ML. After the creation of a composite film, the sample was heated via a linear temperature ramp (1 K/s) to and then held at the isothermal temperature of interest. A Bruker Vertex 70 FTIR was used for the RAIRS experiments. The infrared beam was incident on the sample at an angle of 82° ± 1° from normal and the spectra were acquired with a resolution of 8 cm^{-1}. In the isothermal experiments, we trigger the collection of infrared spectra at 125 K on the temperature ramp which we define as $t = 0$. This results in the first spectrum in a time series to be from a completely amorphous film. However, the first few subsequent spectra may be acquired over a range of temperatures before the final isothermal temperature is reached.

III. RESULTS

A. Crystallization kinetics in capped ASW films on an ice template

In this section, we study the crystallization kinetics of ASW films deposited on a 50 ML crystalline ice (CI) template and then capped with 50 ML of decane. As we have recently shown and demonstrate below, the decane cap layer acts to minimize ice nucleation at the outer surface/vacuum interface.[33,34]

The method used to analyze the crystallization kinetics for all of the results in this paper is illustrated in Fig. 1. The spectra in Fig. 1 are for 500 ML of ASW (5% D_2O in H_2O) that was deposited on 50 ML of crystalline ice and then capped with 50 ML of decane. The film was deposited at ~25 K and then heated to and held at 150 K. RAIRS spectra were averaged and acquired in 9 s intervals during the isothermal annealing. Figure 1 displays a time series of RAIRS spectra for the OD stretching region of HOD. The initial spectrum (red curve) is from the initially amorphous film which eventually transforms into a completely crystallized film (blue curve) with a peak at ~2426 cm^{-1}. The spectra acquired between these times are analyzed to determine the crystallization kinetics. There is an isosbestic point in the spectra which indicates a transformation from one state (amorphous) to another (crystalline).[28,29] The fraction of the film crystallized was determined from the ratio of the absorbance at 2426 cm^{-1} for each spectrum in the series to the absorbance difference between the fully amorphous and crystalline spectra at 2426 cm^{-1}. The analysis was done at 2426 cm^{-1} instead of at 2430 cm^{-1}, the peak of the crystalline spectrum, because the change in absorbance at 2426 cm^{-1} was larger than that at the peak.

Figure 2 displays the experimental results for ASW films with various thicknesses (100, 200, 500, and 1000 ML) deposited on a CI template and capped with decane. The films were deposited at 25 K and linearly heated to and held at 150 K. Figure 2(a) displays a plot of the fraction crystallized vs time. For all thicknesses, the crystallization begins at the onset ($t = 0$) and the fraction crystallized increases linearly with time. For films without a CI template, there is typically an induction time before the onset of crystallization and the fraction crystallized curves have a sigmoidal shape.[9,17,33,34] The preexisting ice template in the current experiments greatly accelerates

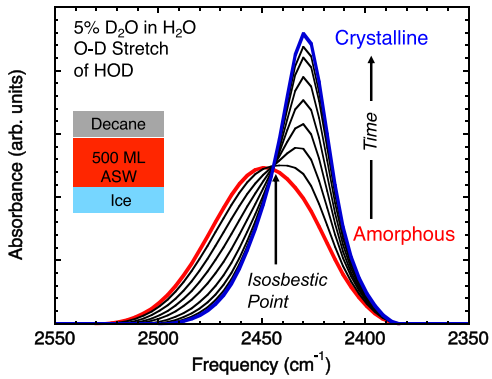

FIG. 1. Time series of RAIRS spectra obtained from a 500 ML thick ASW film (5% D_2O in H_2O) deposited on a 50 ML crystalline ice template and then capped with 50 ML of decane. The films were deposited at 25 K and then heated to and held at 150 K. Displayed is the O-D stretching region for HOD. The red curve is the spectrum from a 100% amorphous film, and the blue curve is the spectrum from a 100% crystalline film. The time difference between the amorphous (red curve) and crystalline (blue curve) spectra is about 300 s.

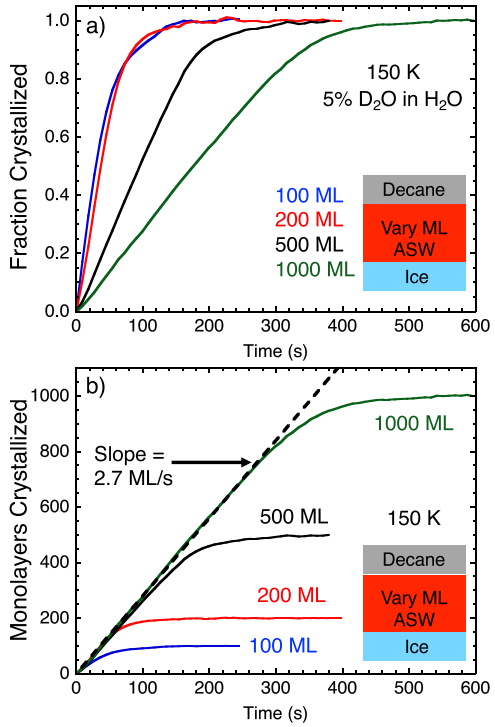

FIG. 2. (a) Fraction crystallized vs time curves for ASW (5% D_2O in H_2O) films on a 50 ML crystalline ice template and capped with 50 ML of decane obtained from isothermal RAIRS experiments at 150 K. The ASW film thicknesses were 100 (blue curve), 200 (red curve), 500 (black curve), and 1000 ML (green curve). (b) A plot of the number of monolayers crystallized vs time for the isothermal experiments at 150 K displayed in (a). The dashed line is a fit to the initial linear part of the curve for the 1000 ML film and yields a crystalline ice growth rate of 2.7 ML/s.

the crystallization kinetics. For example, it took only 350 s for 90% of the 1000 ML film to crystallize [Fig. 2(a), green line]. In contrast, in a previous publication where the ice template was replaced with a decane layer, it took more than 2000 s to crystallize 90% of a 1000 ML film at 150 K.[34] The thickness dependence of the crystallization kinetics observed in that earlier study argued against a random bulk nucleation and growth mechanism,[33,34] and the fast crystallization kinetics observed here for ASW films grown on crystalline ice templates also precludes significant contributions from bulk nucleation and growth.

The results in Fig. 2(a) also show that the time to completely crystallize the film increases with thickness. However, that increasing time is simply related to the increasing film thickness. The RAIRS technique probes the entire film, and as we have shown in prior work, the thickness dependence of the crystallization kinetics argues against a random bulk nucleation and growth mechanism.[33,34] Figure 2(b) displays the results from Fig. 2(a) plotted as the number of monolayers crystallized vs time. In this plot, the curves initially align onto a single line and then saturate at a time that increases with the film thickness. The lack of an induction time and the linear increase in monolayers crystallized with time are consistent with a growth dominated crystallization mechanism. In this case, the CI template bypasses the nucleation step and the observed crystallization is due to crystalline growth that begins at the CI template and moves upward through the ASW overlayer. The crystalline ice growth rate is determined from the slope of the number of monolayers crystallized vs time line. The dashed line is a fit to the initial linear part of the curve for the 1000 ML film and yields a crystalline ice growth rate of ~2.7 ML/s.

Experiments using the same film configuration (ASW on a CI template and capped with decane) were conducted for 200 ML ASW films over a range of isothermal temperatures. Figure 3(a) displays the fraction crystallized vs time at isothermal temperatures from 140 to 148 K. The results show that the time to fully crystallize the ASW film increases with decreasing temperature. Figure 3(b) is a plot of the results from Fig. 3(a) (open symbols) plotted as the number of monolayers crystallized vs time. The data points increase linearly over the displayed range from 20 to 150 ML crystallized. We limit our analysis to the first 150 ML crystallized for the following reason. As shown in Figs. 2 and 3(a), the crystallization rate "turns over" (decreases) as the film approaches complete crystallization. This is

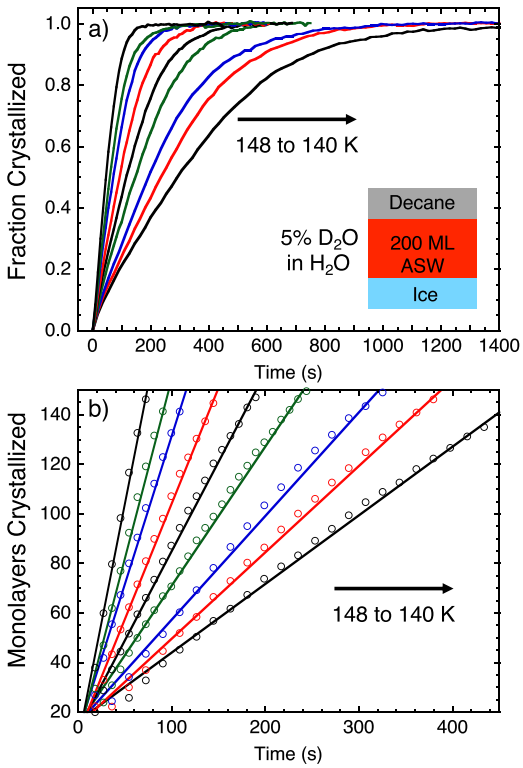

FIG. 3. (a) Fraction crystallized vs time for 200 ML ASW (5% D_2O in H_2O) films deposited on a CI template and capped with decane for a range of isothermal temperatures from 140 to 148 K. (b) Plot of the number of monolayers crystallized (open symbols) vs time for the experiments in (a). The solid lines are linear fits to each isothermal dataset. The slopes from the fits yield the crystalline ice growth rates for CI templated and capped films.

likely due to nonuniformity in the heights that exist in the original, or arise during the growth of, the template layer. Obviously, a perfectly planar template is not expected as AFM images of crystalline ice surfaces have shown.[39,40] We also excluded the data points acquired before ~30 s. As described above, we start the data acquisition at 125 K on the heating ramp. During the time interval before the final isothermal temperature is reached, some crystallization can occur which is not related to the growth rate at the final isothermal temperature. The solid lines are fits to the data points from which the temperature dependent crystalline ice growth rates were determined. The crystalline ice growth rates will be given later in this paper.

B. Crystallization kinetics in uncapped ASW films

In this section, we compare the crystallization kinetics of capped and uncapped ASW films deposited on a 50 ML crystalline CI template. We then use the selective placement of an isotopic layer (5% D_2O in H_2O) to measure the crystalline ice growth rates in uncapped ASW films without a CI template.

Figure 4 is a plot of the number of monolayers crystallized vs time for ASW films with various thicknesses (100, 200, 500, and 1000 ML) deposited on a CI templated without a decane cap. The films were deposited at 25 K and linearly heated to and held at 150 K. The results show that crystallization begins at $t = 0$ and the number of monolayers crystallized initially increases linearly with time for all thicknesses. However, in contrast to the capped film results [see Fig. 2(b)], the crystalline ice growth rates (the slope of the curves) eventually increase above the initial growth rate. The dashed line is a fit to the initial linear part of the 1000 ML curve, which yields a crystalline ice growth rate of ~2.7 ML/s. Hence, the initial crystalline ice growth rates for templated capped [Fig. 2(b)] and uncapped films (Fig. 4) are the same.

To further explore the differences between the crystallization kinetics in capped and uncapped films, the 150 K isothermal crystallization results for the 1000 ML films in both configurations are displayed in Fig. 5. At early times (t < 100 s), the capped (solid line) and uncapped (dashed line) results are aligned with a slope of 2.7 ML/s. At ~100 s, the uncapped film curve deviates upward from the capped curve and eventually increases linearly with a slope of ~5.4 ML/s. The factor of two increase in the crystalline growth rate in the uncapped film suggests that a second crystalline ice template has formed on top of the film. This is consistent with are our previous results for nontemplated ASW films where we showed that nucleation at the vacuum/film interface was more facile than in the bulk.[33,34] In that work, we hypothesized that, after the initial surface nucleation step, a thin crystalline skin or crust forms across the surface of the film and then acts as a template for a growth front that propagates into the bulk.

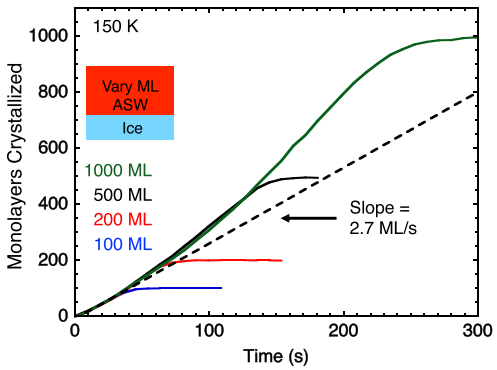

FIG. 4. The number of monolayers crystallized vs time for ASW films with various thicknesses (100, 200, 500, and 1000 ML) deposited on a 50 ML CI template without a decane cap. The films were deposited at 25 K and linearly heated to and held at 150 K. The dashed line is a fit to the initial linear part of the 1000 ML curve which yields a crystalline ice growth rate of ~2.7 ML/s.

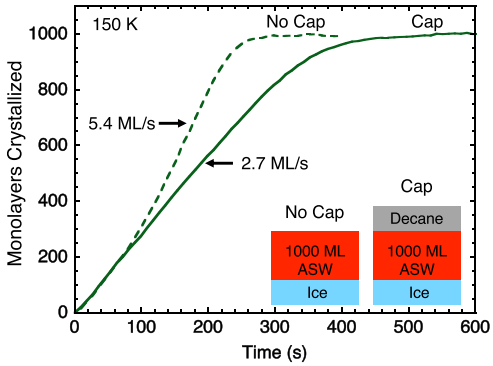

FIG. 5. The number of monolayers crystallized vs time for 1000 ML ASW films deposited on a CI template with (solid green line) and without (dashed green line) a decane cap. The films were deposited at 25 K and linearly heated to and held at 150 K.

To test the hypothesis of the creation of a surface CI template, experiments using isotopic layers placed at various positions in an ASW film were conducted. In these experiments, uncapped 1000 ML ASW films were created using a 100 ML thick isotopic layer (5% D_2O in H_2O) and 900 ML of H_2O [see schematic in Fig. 6(a)]. The films were deposited on a 50 ML decane layer to prevent the graphene substrate from acting as a crystallization template. The isotopic layers were placed 0 (green curves), 300 (black curves), 600 (red curves), and 900 ML (blue curves) from the top of the film. The films were then heated to and held at various isothermal temperatures from 142 to 150 K. The results for a few representative isothermal temperatures are displayed in Fig. 6. The results for the 150 K experiments are displayed in Fig. 6(a) and show that the fraction crystallized curves shift to longer times the further the isotopic layer is from the top of the film. Also notice that crystallization does not start at $t = 0$. Instead, there is a delay in the onset of crystallization that increases with the isotopic layer's distance from the top of the film. The same general behavior is observed for the experiments at 148 K [Fig. 6(b)] and 146 K [Fig. 6(c)]. However, at these lower temperatures, the fraction crystallized curves are shifted to longer times.

The results in Fig. 6 support the idea that a crystalline ice template forms on the surface of uncapped ASW films. From those experiments, we can extract the crystalline ice growth rate from the

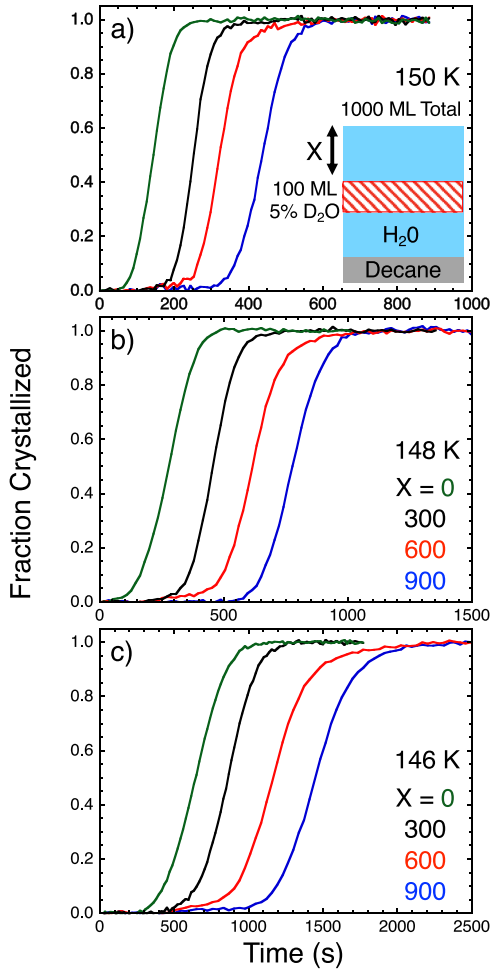

FIG. 6. The fraction crystallized vs time for uncapped 1000 ML ASW films composed of a 100 ML thick isotopic layer (5% D_2O in H_2O) and 900 ML of H_2O deposited on a decane layer. The 100 ML isotopic layer was placed at 0 (green curves), 300 (black curves), 600 (red curves), and 900 ML (blue curves) from the top of the film. Displayed are the results for isothermal experiments at (a) 150 K, (b) 148 K, and (c) 146 K.

surface template. Figure 7 displays a plot of the number of monolayers (50, 350, 650, and 950 ML, i.e., the middle of the isotopic layer) crystallized (solid symbols) vs the crystallization half-times for the results in Fig. 6 and other isothermal temperatures (not shown in Fig. 6). The solid lines are linear fits to the data points and the slopes yield the crystalline ice growth rates which will be discussed in Sec. III C.

C. Crystalline ice growth rates

Figure 8 is an Arrhenius plot of the growth rates obtained for both the CI-templated/capped (red solid circles, obtained from the data in Fig. 3) and nontemplated uncapped (blue solid circles, obtained from the data in Fig. 7). The ice growth rates from

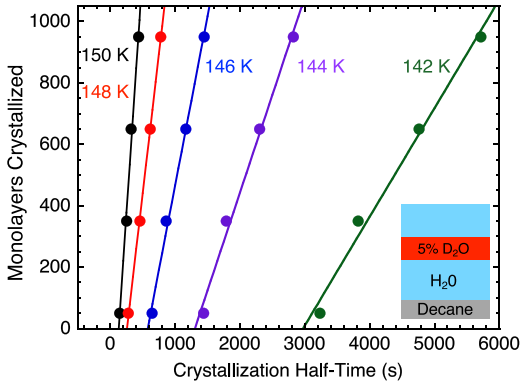

FIG. 7. The number of monolayers (50, 350, 650, and 950 ML) crystallized (solid symbols) vs crystallization half-times for the results in Fig. 6 and other temperatures (not shown in Fig. 6). The solid lines are linear fits to each isothermal dataset and the slopes yield the crystalline ice growth rates for uncapped films.

the two film configurations are in excellent agreement differing by no more than 30% over the temperature from 142 to 150 K. Also displayed are recently published isothermal crystalline growth rates obtained using uncapped 25 ML ASW films deposited on a 75 ML crystalline ice template (green solid circles).[12] These results are within a factor of three over the temperature from 140 to 150 K. The dashed lines are Arrhenius fits that yielded growth activation energies of 40 ± 3 kJ/mol for the data presented in this paper and 43 ± 3 kJ/mol for the previously published data.[12]

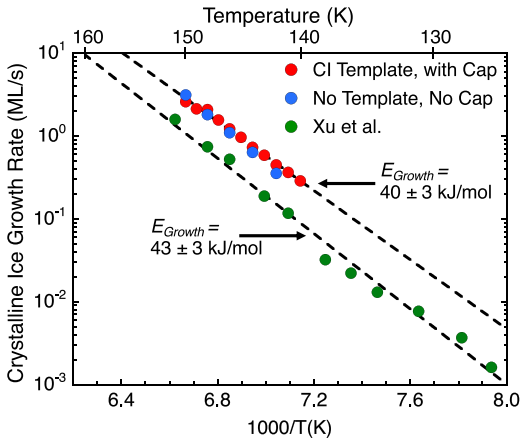

FIG. 8. Arrhenius plot of the crystalline ice growth rate data obtained from the templated/capped experiments in Fig. 3 (red circles) and the nontemplated uncapped experiments in Fig. 7 (blue circles). Also plotted are the crystalline ice growth rate data published in Ref. 12. The dashed lines are Arrhenius fits to the CI-templated/capped data and the data in Ref. 12 which yielded growth activation energies of 40 ± 3 kJ/mol and 43 ± 3 kJ/mol, respectively. The errors are estimated by fitting the data with fixed values of the prefactor that are a factor of 10 higher and lower than the free fit value.

IV. DISCUSSION

In this paper, we measured the crystalline ice growth rates in ASW films in two different composite film configurations. In the first configuration, ASW films were deposited on a crystalline ice template and then capped with decane. These experiments (Figs. 1–3) showed that crystallization begins immediately without an induction period and the fraction of the film crystallized increases linearly with time. The observed kinetics are consistent with crystallization beginning at the ice template/ASW film interface followed by a growth front that propagates upward into the film. Because growth occurs on the ice template, the crystalline ice growth rate is obtained directly from a plot of the number of monolayers crystallized vs time.

The importance and the role of the decane cap layer was demonstrated by comparing the results for capped and uncapped ASW films that were deposited on a crystalline ice template (Figs. 4 and 5). In this case, the crystallization rates for uncapped films are initially the same as those for the capped films but eventually increase above the initial linear ice growth rate. Moreover, the crystalline ice growth rate in the 1000 ML uncapped ASW film eventually reaches a value that is twice that of the capped film. These results indicate that at some point a second crystalline growth front emerges. This is consistent with prior work where we showed that ASW nucleation was more facile at the vacuum interface than in the bulk film.[33,34] We also showed that the presence of a decane cap impedes nucleation at the vacuum interface. We proposed that after surface nucleation in uncapped films, the entire surface crystallizes and a growth front propagates into the ASW film. This model explains the factor of two increase observed in the growth rate in the uncapped film. In uncapped, templated ASW films, the initial crystallization rate is dominated by growth on the CI template. For thicker films, the time to crystallize the film increases and surface nucleation can create a second CI template at the vacuum interface. At this point, there are two crystallization fronts, one moving upward from the original template and a second moving downward from the surface, and this accounts for the factor of two increase in the crystallization rate.

To verify that a crystalline ice template forms across the surface of uncapped films, the crystalline growth rates were measured in a second ASW film configuration. In this case, ASW films were deposited on a decane layer (no CI template) without a decane cap. The selective placement of an isotopic layer at various elevations in a 1000 ML film was used to determine the crystalline ice growth rates. The crystallization kinetics were shown to begin at the film/vacuum interface and propagate linearly into the film (see Figs. 6 and 7). These observations are consistent with a crystalline template forming across the film surface.

The crystalline ice growth rates obtained from ASW films in templated/capped and nontemplated/uncapped configurations are in excellent agreement (Fig. 8). The agreement provides further evidence that a crystalline ice layer forms across the top of the uncapped film. Once formed, the top layer acts exactly as the pregrown crystalline ice template. The growth rate activation energy of 40 ± 3 kJ/mol is in good agreement with the value of 43 ± 3 kJ/mol obtained from recently published data.[12] While our growth rate values are about a factor of three greater than the previously published ones, a shift of 2 K in the temperature would bring the two sets of data to within 30%. A 2 K difference in the temperature calibration between the two separate instruments is not unexpected and is within our absolute temperature error estimates. In addition, the earlier measurements were made with thinner ASW films (25–100 ML) and, as shown in Fig. 2(b), the linearly increasing portion of the crystallization curves will likely be smaller than those for thicker films. As a result, analysis of the growth rates in thinner films could have included more of the nonlinear data range (i.e., data approaching 100% crystallization) resulting in lower growth rates.

The activation energies displayed in Fig. 8 are lower than previously published values of 47 kJ/mol,[26,41] 56 kJ/mol,[24] and 68 kJ/mol.[25] In all of those studies, the crystallization kinetics were measured using the adsorption and desorption of an inert gas on the ASW surface and thus were measuring only the crystallization of the surface layer. In some of those studies, the growth rates were extracted from the crystallization kinetics using random nucleation and growth models.[25,26,41] The higher growth activation energies could be the result of not accounting for surface nucleation in the analysis of the crystallization kinetics.

The crystalline ice growth rates obtained in this work should be useful in estimating bulk nucleation rates from the crystallization kinetics in capped ASW films. Future work will also explore the role of surface nucleation in the crystallization of other amorphous solids including that of methanol and ethanol.

ACKNOWLEDGMENTS

This work was supported by the U.S. Department of Energy (DOE), Office of Science, Office of Basic Energy Sciences, Division of Chemical Sciences, Geosciences, and Biosciences. This research was performed using EMSL, a national scientific user facility sponsored by DOE's Office of Biological and Environmental Research and located at the Pacific Northwest National Laboratory, which is operated by Battelle for the DOE.

REFERENCES

[1] D. A. Williams, W. A. Brown, S. D. Price, J. M. C. Rawlings, and S. Viti, "Molecules, ices and astronomy," Astron. Geophys. **48**, 25–34 (2007).
[2] D. J. Burke and W. A. Brown, "Ice in space: Surface science investigations of the thermal desorption of model interstellar ices on dust grain analogue surfaces," Phys. Chem. Chem. Phys. **12**, 5947–5969 (2010).
[3] P. Jenniskens and D. F. Blake, "Structural transitions in amorphous water ice and astrophysical implications," Science **265**, 753–756 (1994).
[4] P. Jenniskens and D. F. Blake, "Crystallization of amorphous water ice in the solar system," Astrophys. J. **473**, 1104–1113 (1996).
[5] P. G. Debenedetti, *Metastable Liquids: Concepts and Principles* (Princeton University Press, Princeton, NJ, 1996).
[6] P. G. Debenedetti, "Supercooled and glassy water," J. Phys.: Condens. Matter **15**, R1669–R1726 (2003).
[7] C. A. Angell, "Amorphous water," Annu. Rev. Phys. Chem. **55**, 559–583 (2004).
[8] C. A. Angell, "Insights into phases of liquid water from study of its unusual glass-forming properties," Science **319**, 582–587 (2008).
[9] R. S. Smith, N. G. Petrik, G. A. Kimmel, and B. D. Kay, "Thermal and nonthermal physiochemical processes in nanoscale films of amorphous solid water," Acc. Chem. Res. **45**, 33–42 (2012).

[10]K. Amann-Winkel, R. Bohmer, F. Fujara, C. Gainaru, B. Geil, and T. Loerting, "Colloquium: Water's controversial glass transitions," Rev. Mod. Phys. **88**, 011002 (2016).
[11]N. J. Hestand and J. L. Skinner, "Perspective: Crossing the Widom line in no man's land: Experiments, simulations, and the location of the liquid-liquid critical point in supercooled water," J. Chem. Phys. **149**, 140901 (2018).
[12]Y. T. Xu, N. G. Petrik, S. Smith, B. D. Kay, and G. A. Kimmel, "Growth rate of crystalline ice and the diffusivity of supercooled water from 126 to 262 K," Proc. Natl. Acad. Sci. U. S. A. **113**, 14921–14925 (2016).
[13]Y. T. Xu, N. G. Petrik, R. S. Smith, B. D. Kay, and G. A. Kimmel, "Homogeneous nucleation of ice in transiently-heated, supercooled liquid water films," J. Phys. Chem. Lett. **8**, 5736–5743 (2017).
[14]H. Laksmono, T. A. McQueen, J. A. Sellberg, N. D. Loh, C. Huang, D. Schlesinger, R. G. Sierra, C. Y. Hampton, D. Nordlund, M. Beye *et al.*, "Anomalous behavior of the homogeneous ice nucleation rate in 'no-man's land,'" J. Phys. Chem. Lett. **6**, 2826–2832 (2015).
[15]T. S. Li, D. Donadio, and G. Galli, "Ice nucleation at the nanoscale probes no man's land of water," Nat. Commun. **4**, 1887 (2013).
[16]T. S. Li, D. Donadio, G. Russo, and G. Galli, "Homogeneous ice nucleation from supercooled water," Phys. Chem. Chem. Phys. **13**, 19807–19813 (2011).
[17]R. S. Smith, J. Matthiesen, J. Knox, and B. D. Kay, "Crystallization kinetics and excess free energy of H_2O and D_2O nanoscale films of amorphous solid water," J. Phys. Chem. A **115**, 5908–5917 (2011).
[18]P. Lofgren, P. Ahlstrom, D. V. Chakarov, J. Lausmaa, and B. Kasemo, "Substrate dependent sublimation kinetics of mesoscopic ice films," Surf. Sci. **367**, L19–L25 (1996).
[19]P. Lofgren, P. Ahlstrom, J. Lausma, B. Kasemo, and D. Chakarov, "Crystallization kinetics of thin amorphous water films on surfaces," Langmuir **19**, 265–274 (2003).
[20]N. J. Sack and R. A. Baragiola, "Sublimation of vapor-deposited water ice below 170-K, and its dependence on growth-conditions," Phys. Rev. B **48**, 9973–9978 (1993).
[21]R. J. Speedy, P. G. Debenedetti, R. S. Smith, C. Huang, and B. D. Kay, "The evaporation rate, free energy, and entropy of amorphous water at 150 K," J. Chem. Phys. **105**, 240–244 (1996).
[22]R. S. Smith, T. Zubkov, and B. D. Kay, "The effect of the incident collision energy on the phase and crystallization kinetics of vapor deposited water films," J. Chem. Phys. **124**, 114710 (2006).
[23]Z. Dohnalek, R. L. Ciolli, G. A. Kimmel, K. P. Stevenson, R. S. Smith, and B. D. Kay, "Substrate induced crystallization of amorphous solid water at low temperatures," J. Chem. Phys. **110**, 5489–5492 (1999).
[24]Z. Dohnalek, G. A. Kimmel, R. L. Ciolli, K. P. Stevenson, R. S. Smith, and B. D. Kay, "The effect of the underlying substrate on the crystallization kinetics of dense amorphous solid water films," J. Chem. Phys. **112**, 5932–5941 (2000).
[25]D. J. Safarik, R. J. Meyer, and C. B. Mullins, "Thickness dependent crystallization kinetics of sub-micron amorphous solid water films," J. Chem. Phys. **118**, 4660–4671 (2003).
[26]D. J. Safarik and C. B. Mullins, "The nucleation rate of crystalline ice in amorphous solid water," J. Chem. Phys. **121**, 6003–6010 (2004).
[27]E. H. G. Backus, M. L. Grecea, A. W. Kleyn, and M. Bonn, "Surface crystallization of amorphous solid water," Phys. Rev. Lett. **92**, 236101 (2004).
[28]W. Hage, A. Hallbrucker, E. Mayer, and G. P. Johari, "Crystallization kinetics of water below 150 K," J. Chem. Phys. **100**, 2743–2747 (1994).
[29]W. Hage, A. Hallbrucker, E. Mayer, and G. P. Johari, "Kinetics of crystallizing D_2O water near 150 K by Fourier-transform infrared-spectroscopy and a comparison with the corresponding calorimetric studies on H_2O water," J. Chem. Phys. **103**, 545–550 (1995).
[30]T. Kondo, H. S. Kato, M. Bonn, and M. Kawai, "Deposition and crystallization studies of thin amorphous solid water films on Ru(0001) and on CO-precovered Ru(0001)," J. Chem. Phys. **127**, 094703 (2007).
[31]T. Kondo, H. S. Kato, M. Bonn, and M. Kawai, "Morphological change during crystallization of thin amorphous solid water films on Ru(0001)," J. Chem. Phys. **126**, 181103 (2007).
[32]M. T. Sieger and T. M. Orlando, "Probing low-temperature water ice phases using electron-stimulated desorption," Surf. Sci. **451**, 97–101 (2000).
[33]C. Q. Yuan, R. S. Smith, and B. D. Kay, "Surface and bulk crystallization of amorphous solid water films: Confirmation of 'top-down' crystallization," Surf. Sci. **652**, 350–354 (2016).
[34]C. Q. Yuan, R. S. Smith, and B. D. Kay, "Communication: Distinguishing between bulk and interface-enhanced crystallization in nanoscale films of amorphous solid water," J. Chem. Phys. **146**, 031102 (2017).
[35]T. Zubkov, R. S. Smith, T. R. Engstrom, and B. D. Kay, "Adsorption, desorption, and diffusion of nitrogen in a model nanoporous material. I. Surface limited desorption kinetics in amorphous solid water," J. Chem. Phys. **127**, 184707 (2007).
[36]G. A. Kimmel, J. Matthiesen, M. Baer, C. J. Mundy, N. G. Petrik, R. S. Smith, Z. Dohnalek, and B. D. Kay, "No confinement needed: Observation of a metastable hydrophobic wetting two-layer ice on graphene," J. Am. Chem. Soc. **131**, 12838–12844 (2009).
[37]M. Fisher and J. P. Devlin, "Defect activity in amorphous ice from isotopic exchange data—Insight into the glass-transition," J. Phys. Chem. **99**, 11584–11590 (1995).
[38]J. P. Devlin, "Structure, spectra, and mobility of low-pressure ices: Ice I, amorphous solid water, and clathrate hydrates at T < 150 K," J. Geophys. Res.: Planets **106**, 33333–33349, https://doi.org/10.1029/2000je001301 (2001).
[39]K. Thurmer and S. Nie, "formation of hexagonal and cubic ice during low-temperature growth," Proc. Natl. Acad. Sci. U. S. A. **110**, 11757–11762 (2013).
[40]K. Thurmer, C. Q. Yuan, G. A. Kimmel, B. D. Kay, and R. S. Smith, "Weak interactions between water and clathrate-forming gases at low pressures," Surf. Sci. **641**, 216–223 (2015).
[41]D. J. Safarik and C. B. Mullins, "A new methodology and model for characterization of nucleation and growth kinetics in solids," J. Chem. Phys. **119**, 12510–12524 (2003).